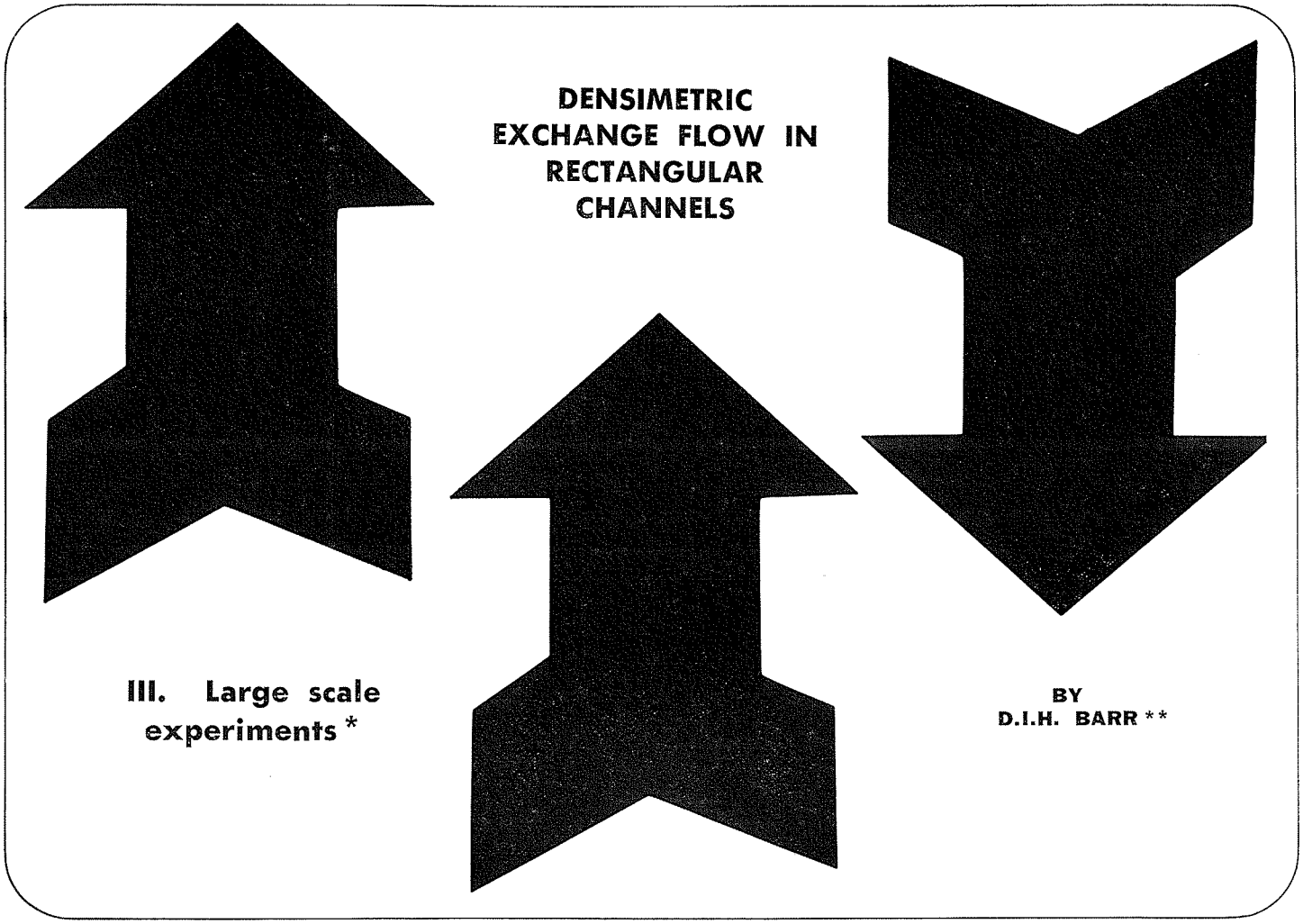

DENSIMETRIC EXCHANGE FLOW IN RECTANGULAR CHANNELS

III. Large scale experiments *

BY
D.I.H. BARR **

Notation

B	flume breadth;
e	vertical exaggeration, x/y;
f	acceleration due to field force;
g	acceleration due to gravity;
g'	reduced acceleration (due to buoyancy);
H	depth of water;
l	representative length generally;
L	horizontal distance;
T	time;
V	velocity;
x	horizontal scale is $1/x$;
y	vertical scale is $1/y$;
ρ	mass density;
μ	viscosity;
ν	kinematic viscosity;
$\Delta\sigma$	surface tension difference.

Subscripts:

$_0$	relating to initial conditions in lock exchange flow;
$_s$	relating to more dense fluid;
$_1$	relating to liquid in lock of circular flume;
$_2$	relating to liquid in main length of circular flume;
$_\Delta$	densimetric dynamic;
$_\nu$	viscous dynamic;
$_r$	resultant;
$_{\Delta\sigma}$	differential surface tension dynamic;
$_m$	model;
$_p$	prototype.

Introduction

This is the third paper under the main title. The previous papers will be referred to as I [1] and II [2]. In I the background to the studies was introduced at some length. It was said that densimetric exchange flow was of interest *per se*, as a phenomenon which exhibited a considerable range of viscous scale effect and, further, that knowledge of exchange flow as it occurs in idealised circumstances could be used to obtain the best choice of vertical exaggeration for certain types of hydraulic model where density spread phenomena were to be simulated.

In the main some familiarity with I and II will be assumed. Included in II was reference to the intention to deal with the arrested wedge phenomenon in the third paper as compared with the lock exchange case which was the subject of I and

* Part I and II of this series were published in No. 7/1963 of *La Houille Blanche* (pp. 739-766) (Part I: Definitions, review and relevance to model design. Part II: Some observations of the structure of lock exchange flow.)

** Department of Civil Engineering, University of Strathclyde, Glasgow.

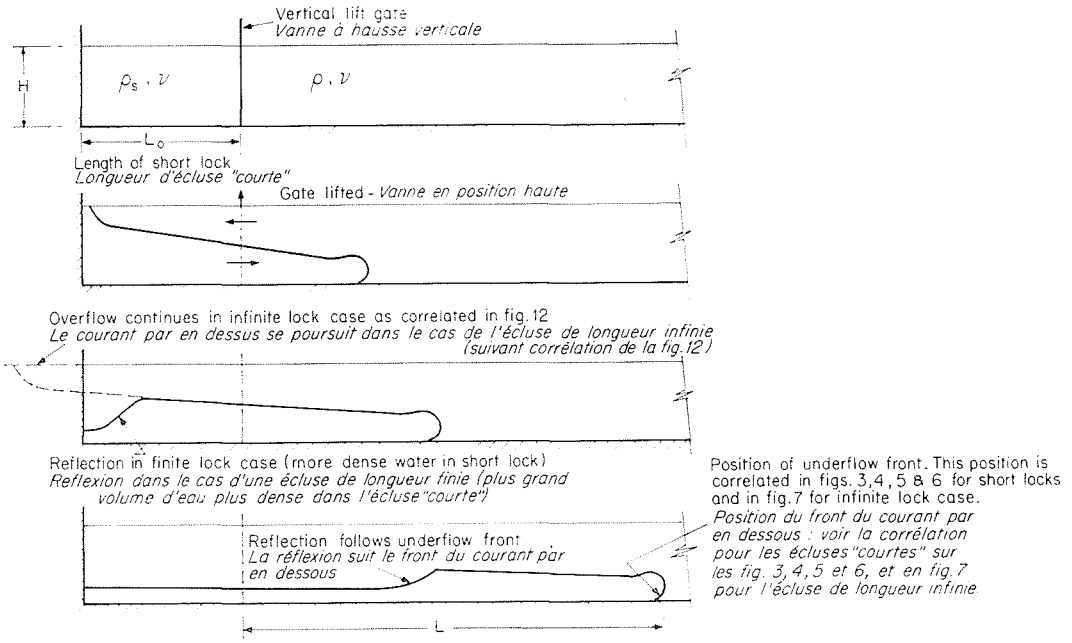

1/ Schematic illustration of lock exchange flow. Short lock underflow case shown.
Représentation schématique du courant consécutif à l'ouverture d'une écluse. Cas du courant par en-dessous dans une écluse « courte ».

II. Lock exchange flow is taken to signify the currents which arise following the removal of the vertical cross-barrier shown in Figure 1. Initially this has separated bodies of still water of differing densities contained in adjoining lengths of the prismatic horizontal bottomed conduit. Arrested wedge phenomena, on the other hand, arise when one body of water makes its way against a normal flow because of small differences in density and where a point of balance is reached. Water is here taken to represent the generality of any liquid or liquids in open conduits and of any fluid in closed conduits. Some work on the arrested wedge was, in fact, undertaken and has, in part, been reported by Majewski [3]. However, the logical sequence of papers in this series has been altered by the recent availability of a specially designed large flume for density current studies, this having been provided under a Science Research Council Grant. The flume is 87.5 m long, 152 cm wide and can be used at depths up to 42 cm. It has been used initially for lock exchange flow experiments—the need for large scale experiments having been stressed at the end of II.

In I the author hypothesised (especially see Fig. 8 of I) that in a lock exchange flow a stage would be reached where changes in viscosity would have no major effect on the phenomenon. Some discussion of the truth or otherwise, of this hypothesis was reported in *La Houille Blanche* [4]. This has further reinforced the desirability of initially utilising the vastly improved facilities for lock exchange studies.

Similarity theory

There are three distinct ways of deriving dimensionless numbers and formulating groupings of dimensionless numbers in similarity equations pertaining to fluid mechanics. Firstly such numbers arise inevitably from complete analytical treatment. By complete analysis is meant a forecast regarding some dependant occurence which is found to be in satisfactory agreement with observation without any empirical interposition whatsoever. Because of the power of dimensionless numbers in respect of the correlation of observations of complex occurrences it is desirable that these be isolated even where complete analysis is not possible. To proceed from the equations of state and of motion and to isolate dimensionless numbers which are thereupon utilised for empirical correlation (if this be done forthrightly) is a useful method and may be termed incomplete analysis. However there are a regrettably large number of instances where the empirical nature of the interposition of constants and adjustments to make theory fit observed data is glossed over. This is better termed pseudo-complete analysis.

The two further methods of the arrangement of variables into dimensionless numbers are by similarity theory giving partial analysis and by dimensional analysis. Prandtl [5] stressed the difference between these, but this distinction is often blurred because of the lack of a complete formal method stemming from physically based similarity theory to set against the mathematically based method of dimensional analysis. The similarity arguments introduced in I represent the initial stages of the devising of a formal similarity method for the arrangement of variables in fluid mechanics, which will be called the method of synthesis.

Density current studies such as those to be described do not present a particularly difficult case in the arrangement of variables but it is desirable to briefly recast the similarity arguments given in I into the new form. The method of synthesis has already been introduced in the context of uniform flow [6, 7], turbo-machines [8], and turbid density currents [9].

Method of synthesis applied to density current phenomena.

A dimensional framework must be chosen. Conventionally, for similarity considerations this is length-mass-velocity, or more precisely length-density-velocity, and this shall be retained, velocity being taken as the primary flow characteristic. The most obvious alternative to velocity is time, and this would be equally suitable, but as we think of, for example, the Froude number as $V/\sqrt{gl}$ and the Reynolds number as Vl/ν it is normally best to retain the velocity as the primary flow characteristic and to make time, acceleration, flow quantity, momentum, energy power and the like, alternative flow characteristics. However the parallel argument for time as primary flow characteristic will also be outlined. This means that dynamic velocities are derived as a measure of the comparative effect of relevant active forces on comparable accelerative systems. As an aside, it should be noted that uniform *laminar* flow in a straight conduit is the only non-accelerative system commonly found. Dynamic velocities are defined as being proportional to the velocity attained if a representative element is acted on by an active force through a representative distance. Suppose the depth, H, in a flume where a lock exchange flow is to be set up is taken as the representative length; the ratio B/H being sufficiently large for side effects to be assumed negligible where B is the flume breadth (Fig. 1). The active force on a representative element is proportional to $(\rho_s - \rho)\, gH^3$ where ρ_s is density of the more dense liquid and ρ that of the less dense liquid. Because the effect of this force on a representative element is different depending whether the element is considered to be of density ρ_s or of density ρ, two dynamic velocities arise by virtue of the density difference, viz. V_Δ and $V_{\Delta s}$, where:

$$V_\Delta = \sqrt{\left[\frac{(\rho_s - \rho)\, gH^3 \times H}{\rho H^3}\right]} = \sqrt{\left(\frac{\rho_s - \rho}{\rho}\right) gH} \quad (1)$$

The $\sqrt{2}$ in:

$$\text{velocity} = \sqrt{2}\sqrt{\frac{\text{force}}{\text{mass}} \times \text{distance}} \quad (2)$$

is omitted because the dynamic velocity concept is to be applied consistently to comparable systems.

Here V_Δ will be written $\sqrt{g'H}$.

$V_{\Delta s}$ is likewise:

$$\sqrt{\frac{\rho_s - \rho}{\rho_s}\, gH}$$

which will be written $\sqrt{g'_s H}$.

To obtain the viscous dynamic velocity V_ν, it is necessary to utilise V_ν on both sides of the defining equation, because viscous force cannot initiate motion.

Then:

$$V_\nu = \sqrt{\frac{\mu V_\nu H \times H}{\rho H^3}} \quad (3)$$

$$\therefore V_\nu = \nu/H \quad (4)$$

where μ is the viscosity and $\nu = \mu/\rho$.

In theory, there would be $V_\nu = \nu/H$ and $V_{\nu s} = \nu_s/H$, where $\nu_s = \mu/\rho_s$. However for the case in hand $\nu \doteqdot \nu_s$, and while both V_Δ and $V_{\Delta s}$ are definite requirements within practical limits this is not so for V_ν and $V_{\nu s}$.

In the case of lock exchange flow there is no velocity or other flow characteristic independently imposed on the system. Thus the relationship between V_Δ, $V_{\Delta s}$ and V_ν defines the system (assuming B to be much greater than H) and that geometrical similarity otherwise obtains.

If V_r is a resultant velocity, suitably defined,

$$\Phi\,(V_r, V_\Delta, V_{\Delta s}, V_\nu) = 0 \quad (5)$$

is the fundamental similarity equation, and a suitable non-dimensional arrangement is:

$$\frac{V_r}{V_\Delta} = \Phi\left(\frac{V_\Delta}{V_\nu}, \frac{V_{\Delta s}}{V_\Delta}\right) \quad (6)$$

which written more completely is:

$$\frac{V_r}{\sqrt{g'H}} = \Phi\left(\frac{(g')^{1/2}\, H^{3/2}}{\nu}, \frac{\rho}{\rho_s}\right) \quad (6\,a)$$

Had the first choice been to work in a length-density-time framework, an equation of the same form as Eq. (5) would have been obtained, consisting largely of dynamic times—the time interval for a representative element to move from rest through a representative distance under an active force.

It will be seen that there is not any essential difference in the class of non-dimensional groups which do not contain actual flow characteristics, whatever the choice of primary flow characteristic. For instance, $\sqrt{gH}$ is the basic form of gravitational dynamic velocity and ν/H likewise the basic form of viscous dynamic velocity. The ratio reduces to $g^{1/2}\, H^{3/2}/\nu$. Gravitational dynamic time in basic form is $\sqrt{H/g}$ and viscous dynamic time is H^2/ν, giving the same form of ratio $g^{1/2}\, H^{3/2}/\nu$.

Surface tension effects and surface waves.

To correlate surface tension modifications of the overflow front, the differential surface tension dynamic velocity is derived:

$$V_{\Delta\sigma} = \sqrt{\frac{\Delta\sigma H \times H}{\rho H^3}} = \sqrt{\frac{\Delta\sigma}{\rho H}} \quad (7)$$

where $\Delta\sigma$ is the difference in surface tension between the bodies of water. This is most logically combined with $\sqrt{g'H}$ to give a further non-dimensional number $(g')^{1/2}\, H\rho^{1/2}/(\Delta\sigma)^{1/2}$ which would be inserted in Eq. (6 *a*), if the movement of the overflow front was to be studied at small scales.

In the studies to be reported the problem of surface tension effects was avoided so far as possible. It was not possible, however, to avoid the influence of surface disturbances. The standard gravitational dynamic velocity based on the depth of water as representative length is obtained in the manner already demonstrated as $\sqrt{gH}$. This when

combined with $\sqrt{g'H}$ gives, $(\rho_s - \rho)/\rho$ as an additional term to be entered in Eq. (6 *a*), i.e.

$$\frac{V_r}{\sqrt{g'H}} = \Phi\left(\frac{(g')^{1/2}\,H^{3/2}}{\nu}, \frac{\rho}{\rho_s}, \frac{\rho_s - \rho}{\rho}\right) \qquad (6\,b)$$

It will be seen that the second and third terms on the right hand side of Eq. (6 *b*) convey the same information, but with differing significance. If ρ and ρ_s are similar, the halving of $\rho_s - \rho$ makes little difference to ρ/ρ_s but naturally halves the value of $(\rho_s - \rho)/\rho$. Where applicable the requirement of constancy of $(\rho_s - \rho)/\rho$ is thus much more stringent. In tidal models for instance, it is essential to adopt the same density difference in the model as obtains in the prototype. Superficially, then, it appears that the addition of the third term merely expresses the greater need to maintain constancy of ρ/ρ_s where free surface disturbances are present, but on further thought the redundancy of definition thus added to the parametric right hand side of Eq. (6 *b*) apparently represents a failure in the method of synthesis. This is because the circumstance of density currents is a particular and restricted case of a generality albeit the case of overwhelming practical significance. Returning to the hypothetical case, introduced in I, of submerged ferrous bodies where the effective body force may be rendered independant of gravity and of the relation of the mass densities by a variable magnetic field, suppose that a submerged body is initially held below the surface of deep water and the submerged weight plus magnetic field force is defined by an (computed) acceleration f. It surface wave effects are to be expected on release of the body the three defining dynamic velocities can be found to be:

$$\sqrt{fl} \qquad \sqrt{(\rho_s/\rho)\,fl} \qquad \text{and} \qquad \sqrt{gl}$$

where ρ_s is here taken as the density of the body, ρ that of the water and l is the representative size of the object to which the submergence is also scaled. These give groups:

$$\rho/\rho_s \qquad \text{and} \qquad f/g$$

which represent the most general form of the third and fourth groups of Eq. (6 *b*). It will be seen that the groups can be controlled independantly in hypothesis and that constancy of both groups would, *inter alia*, be required for dynamical similarity.

The possibility of density currents in magnetic fluid systems [10] introduces even further complications. For the present, mention will be made of some preliminary experiments designed to explore the relevance of the ρ/ρ_s correlation of Eq. (6 *b*) to the main series of experiments.

Exchange flow in circular conduit.

A perspex tube 14.3 cm in diameter was fitted with a gate and used for short lock exchange flow experiments. Because the tube was always full, the $(\rho_s - \rho)/\rho$ term of Eq. (6 *b*) can be neglected. Because in the circumstance of use of water of more or less constant viscosity, and a single size of conduit the term $(g')^{1/2}\,H^{3/2}/\nu$ of Eq. (6 *b*) varies over a fairly small portion of its relevant range with change in g', this too can be ignored for the purpose in hand. In fact, the most significant results, as shown in Figure 2, were for tests at almost the same values of $(g')^{1/2}\,H^{3/2}/\nu$ because the cross sectional symmetry of the tube allowed overflow to be compared with underflow and thus the effective range of ρ/ρ_s obtained was from 0.838 to 1.20. Instead of plotting:

$$\frac{V_r}{\sqrt{g'H}} = \Phi\left(\frac{\rho}{\rho_s}, \frac{L}{H}\right)$$

where L/H is the relative distance at which V_r is observed, the time form of densimetric Froude number has been adopted, that is the plot is based on:

$$\frac{T}{\sqrt{H/g'}} = \Phi\left(\frac{\rho}{\rho_s}, \frac{L}{H}\right) \qquad (8)$$

where T is the elapsed time from the removal of the barrier till point L/H is reached by the front. In the circumstances the notation ρ_1 has been used for the density of the fluid initially in the short lock, whose movement is correlated, and ρ_2 for the fluid initially in the longer length, irrespective of whether:

$$\rho_1 > \rho_2 \qquad \text{or} \qquad \rho_1 < \rho_2$$

It will be seen that the ρ/ρ_s correlation can just be distinguished. For the main series of test the range of ρ/ρ_s was from 1.0 to 1.1, approximately

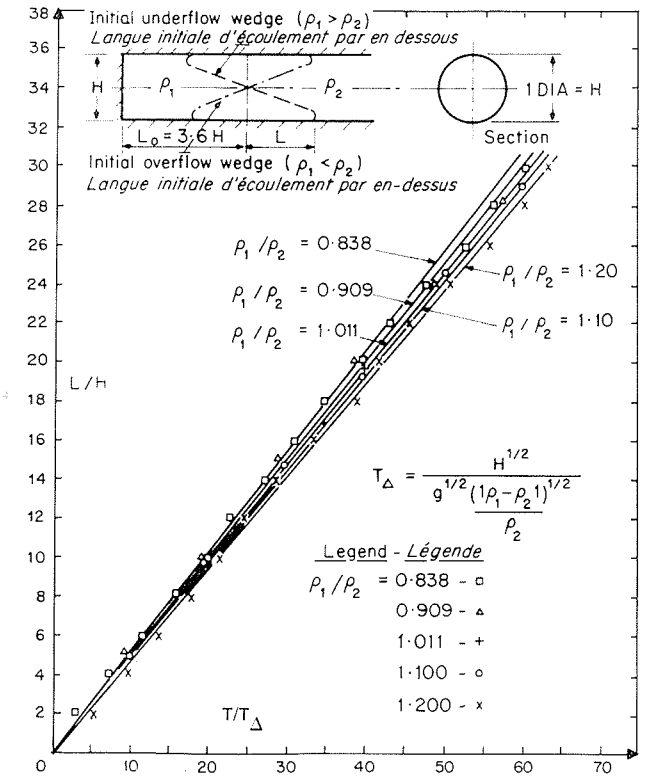

2/ Results of circular flume experiments showing slight density ratio correlation.
Résultats d'essais en canal circulaire, mettant en évidence une légère corrélation du rapport des densités.

New congruency diagram for underflow in wide flume.

Nouveau schéma de congruence, pour le cas du courant par en-dessous dans un canal de grande largeur.

3/ $L_0/H = 14.4$.

4/ $L_0/H = 7.2$.

5/ $L_0/H = 3.6$.

6/ $L_0/H = 1.8$.

7/ No reflection case.
Sans réflexion.

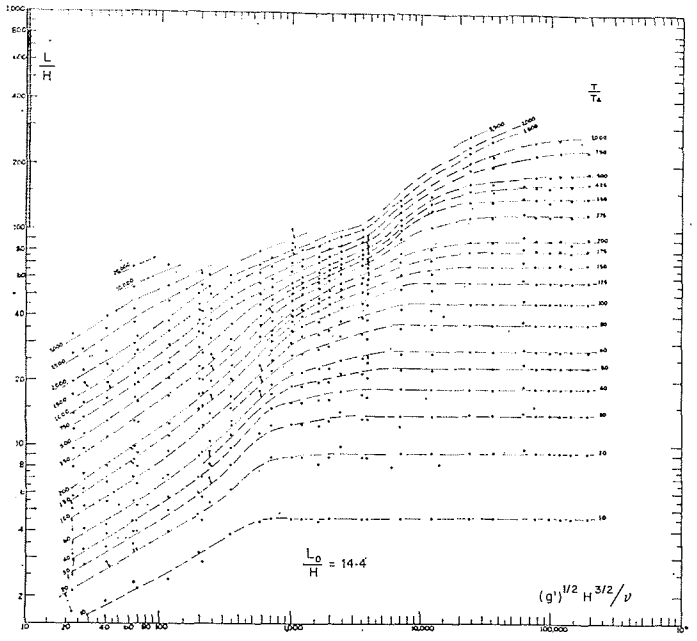

3/

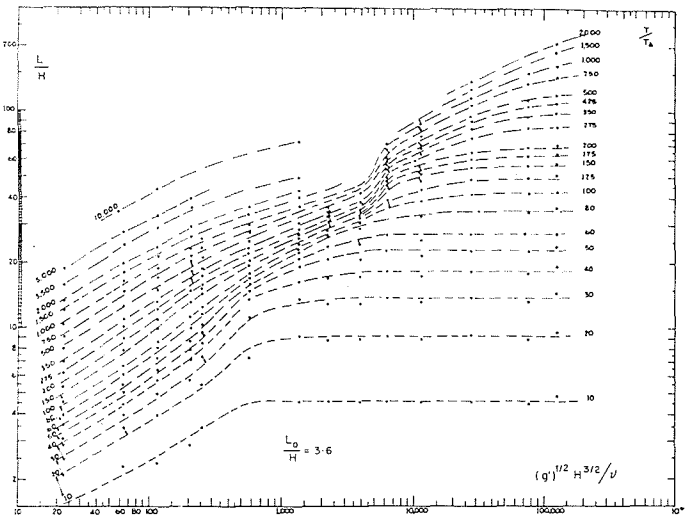

5/

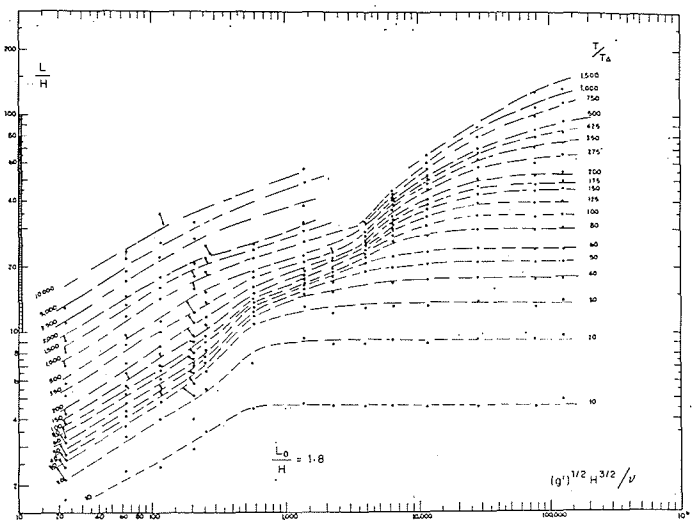

6/

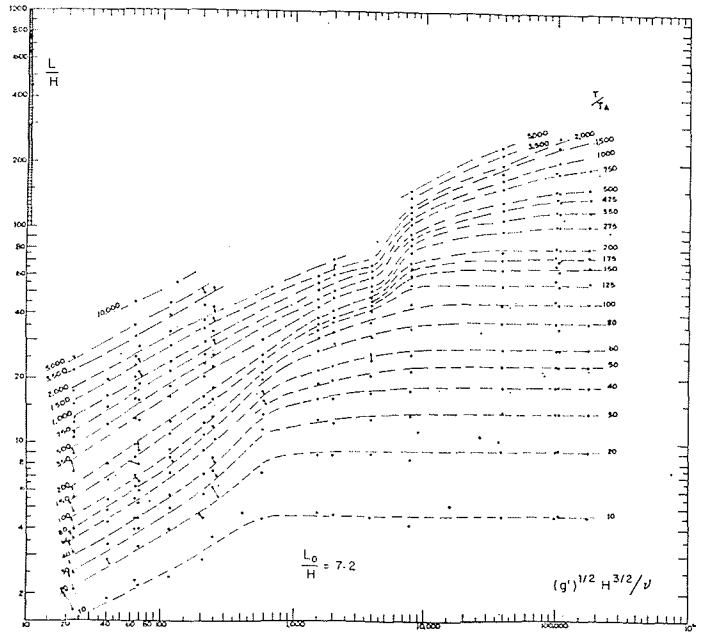

4/

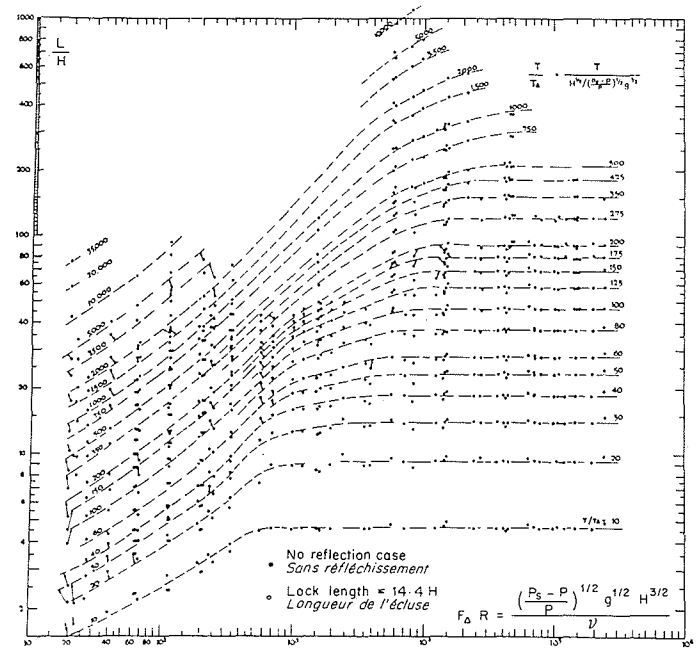

7/

New congruency diagram for overflow in vide flume.

Nouveau schéma de congruence pour le cas du courant par en-dessus dans un canal de grande largeur.

8/ $L_0/H = 14.4$.

9/ $L_0/H = 7.2$.

10/ $L_0/H = 3.6$.

11/ $L_0/H = 1.8$.

12/ No reflection case.
Sans réflexion.

8/

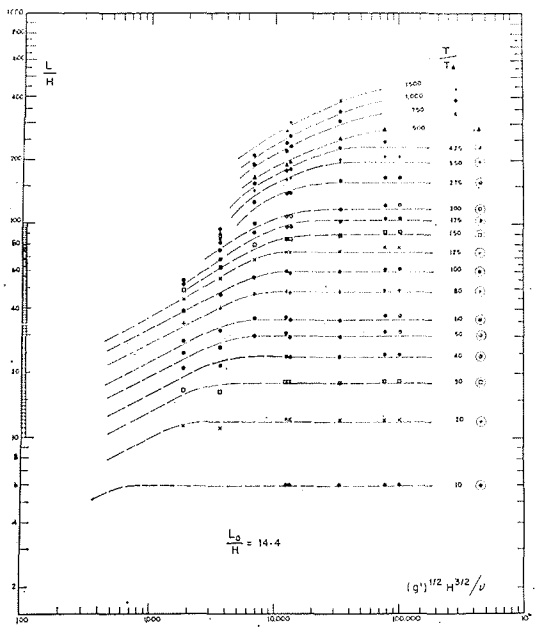

9/

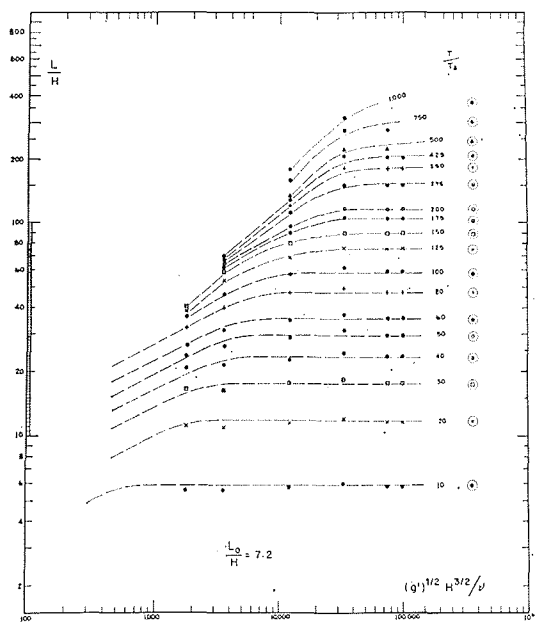

10/

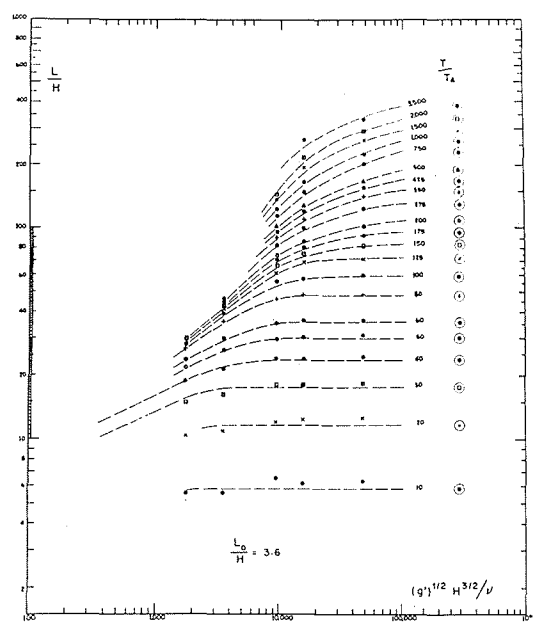

11/

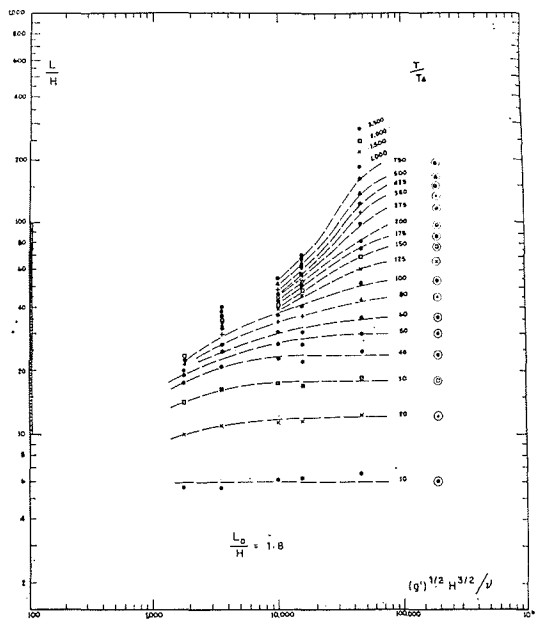

12/

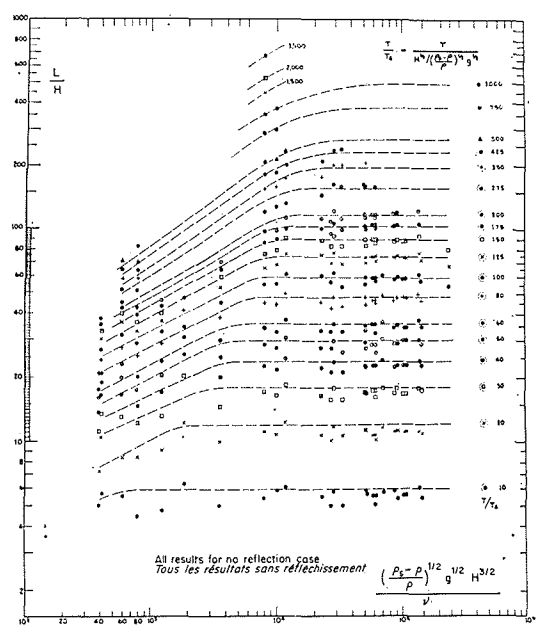

one quarter of the range required to show significant correlation in Figure 2. Thus it was considered reasonable to ignore the ρ/ρ_s correlation.

Main test series

Short lock underflow experiments.

Keulegan [11] has described a comprehensive series of experiments relating to the underflow from short locks. He adopted lock lengths such that L_0/H was either 7.2 or 14.4, and concentrated on tests where the relative width B/H, was about 0.5, B being the flume breadth. However he also demonstrated that the effect of relative width became indistinguishable for B/H values greater than about 4. As indicated above, Keulegan always placed the more dense water in the short lock and observed the underflow as it progressed along the remainder of the flume. It was thought desirable by the present author, to first form a new congruency diagram for the Keulegan configuration of $L_0/H = 14.4$, but with $B/H \geqslant 3.5$.

With a depth of 42 cm, and maximum values of $\rho_s - \rho$ of about 0.1 gm/m.l, as stipulated by the requirement that the ρ/ρ_s correlation would be ignored, a maximum value of densimetric Froude-Reynolds number, $(g')^{1/2} H^{3/2}/\nu$ of 231,000 was obtained, with an available relative extension of 192. With the short lock ($L_0/H = 14.4$), the effect on the front velocity of surface surges was slight, but sufficiently discernable to cause difficulties if strict adherence to the following equation were attempted:

$$\Phi\left(\frac{V_r}{\sqrt{g'H}}, \frac{(g')^{1/2} H^{3/2}}{\nu}, \frac{L}{H}\right) = 0 \qquad (9)$$

Eq. (9) is based on Eq. (6 *a*) with V_r defined as front velocity at relative extension L/H. It would, however, have to be relatively easy to adopt a smoothed value of V_r, but it was considered that greater physical significance would be displayed on the final congruency diagrams by instead adopting T as the dependent variable for the experiments i.e.:

$$\Phi\left(\frac{T}{\sqrt{H/g'}}, \frac{(g')^{1/2} H^{3/2}}{\nu}, \frac{L}{H}\right) = 0 \qquad (10)$$

where T is the smoothed value of elapsed time for the front to reach relative extension L/H. The derivation of Eq. (10) is implicit in the previous discussion of dynamic time. Alternatively, if velocity form is required for the dimensionally homogeneous equation, Eq. (10) can be seen to arise from an arrangement of :

$$\Phi\,(H/T, (g')^{1/2} H^{1/2}, \nu/H) = 0 \qquad (11)$$

together with non-dimensional definition of point of observation, L/H. Figure 3 shows the results obtained utilising the 87.5 m flume for the tests at higher values of $(g')^{1/2} H^{3/2}/\nu$. For lower values of $(g')^{1/2} H^{3/2}/\nu$, the flumes B and C (as described in II) were used. Flume C was 0.635 cm deep, and being enclosed gave a double 'underflow'. To further increase the range of values of $(g')^{1/2} H^{3/2}/\nu$, sugar solutions were also adopted as the basic fluid, with salt added to provide density difference. In the diagrams lines of constant value of non-dimensional time, $T/(H/g')^{1/2}$ (written T/T_Δ on the diagrams), have been plotted against abscissa of $(g')^{1/2} H^{3/2}/\nu$ and ordinate of L/H.

It will be recalled that one main objective of the test programme was to obtain scaling rules for hydraulic models, in particular to provide a rational basis for choice of vertical exaggeration. The effect of vertical exaggeration on the short lock length circumstance, would be to reduce in absolute terms the value of L_0/H. Thus it was thought suitable to also adopt Keulegan's second value of L_0/H, i.e. 7.2, and further to conduct tests at L_0/H values of 3.6 and 1.8. This gave coverage for vertical exaggerations up to 8. The diagrams for L_0/H values of 7.2, 3.6 and 1.8 are shown in Figure 4, 5 and 6 respectively. In Figures 3, 4, 5, 6 experimental points pertain to the nearest line except in a few cases where arrows are used for identification.

Underflow experiments with barrier at approximateiy mid-point of flume.

Alternative to the short lock underflow experiments, where the reflection of the overflow front has sooner or later a manifest effect on the progress of the underflow front, experiments were also conducted with the removeable barrier positioned near the mid-point of the flume length, so as to avoid the effect of reflection of the overflow within the period of observation. There will be discussion of the possible effect of surface surges on such experiments later in the paper; for the present the results are shown in Figure 7.

There was a common initial plot of the data on which Figure 3, 4, 5, 6 and 7 were based. These diagrams are thus compatible over those relative distances, L/H, where there is no influence of reflection and should be considered together as a whole.

Overflow experiments.

Free surface overflow experiments were undertaken for the same configurations as for the under flow and results are given as follows: Figures 8, 9, 10 and 11 for short locks with L_0/H values of 14.4, 7.2, 3.6 and 1.8 respectively; Figure 12 for barrier near mid-point of flume (no reflection case). Again the diagrams originate from a common initial plot and are compatible outwith the zones of influence of reflection. The overflow experiments were performed subsequent to the underflow experiments and there is some dependence in the general runs of the lines of equal value of T/T_Δ from those of the underflow diagrams. The range of values of $(g')^{1/2} H^{3/2}/\nu$ is smaller than for the underflow tests because there was no possibility of an equivalent to the double underflow tests using the 0.635 cm deep flume C. In general there is much greater difficulty in obtaining good overflow results at small values of $(g')^{1/2} H^{3/2}/\nu$ than for comparable underflow results because of the interacting influences of differential surface tension, of surface tension effects on the sides of the flume, and of surface scum effects which are almost unavoidable in normal laboratory conditions.

Initial assessment of new diagrams

Initial velocities.

Insofar as the standard case of the rectangular flume is concerned it is shown that, outwith the range of viscous influence, the initial velocities of the fronts, V_0, are related to the densimetric velocity as follows:

Underflow:

$V_0 = 0.465\ V_\Delta$, i.e. $L/H = 4.65$ at $T/T_\Delta = 10$

Overflow: $V_0 = 0{,}59\ V_\Delta$

The new diagrams show that the supposed trends of slow variation of the coefficients of proportionality as above with $(g')^{1/2}\ H^{3/2}/\nu$ (see Fig. 2 of I) have been the result of systematic error arising from small apparatus and inadequate methods of correlation.

Onset of Froudian conditions.

Confirmation has been obtained of author's hypothesis of onset of Froudian conditions wherein a small change in value of viscosity does not affect the overall behaviour. In fact, the more significant method of correlation indicates that there was little reason for dubiety in the matter.

Diminution of velocity in no-reflection cases (Fig. 7 and 12).

The log — log presentation of the diagrams allows effective demonstration of the great modifications which are brought about by viscous scale effect. Data in this region may primarily serve as a warning of the impossibility of operation of small scale models without vertical exaggeration. There is very definite evidence on the diagrams that the extent of relative extension under Froudian conditions increases with increasing value of:

$$(g')^{1/2}\ H^{3/2}/\nu.$$

In the zone of Froudian conditions, the initial uniformity of the front velocity is marked—for the underflow the averaged value of L/H is 4.65 for $T/T_\Delta = 10$ and is 46.5 for $T/T_\Delta = 100$. Figure 13 shows a natural plot of averaged values of L/H against T/T_Δ for the Froudian zone. For the underflow a very slight extrapolation on Figure 7 indicates that for $T/T_\Delta = 1{,}000$ the value of L/H is 390 which gives a front velocity at that point of $V = 0.36\ V_\Delta$. Rather greater extrapolation indicates that for $T/T_\Delta = 10{,}000$ the value of L/H would be about 3,000 with $V = 0.26\ V_\Delta$, and that at such extensions Froudian conditions would be attained at values of $(g')^{1/2}\ H^{3/2}/\nu \geqslant 10^6$. It is emphasised that these latter figures are based on extrapolation, but it can be seen that in the event of the figures being significantly in error the correctly extended diagram (Fig. 7) must necessarily show some marked discontinuity from the pattern actually established.

Diminution of velocity in short lock cases (Fig. 3, 4, 5, 6, 8, 9, 10 and 11).

In the Froudian zone, it is perhaps surprising to find that at non-dimensional time T/T_Δ of 100, there is no difference in the relative distance travelled by the fronts in the cases of no-reflection, and of L_0/H values of 14.4 and 7.2, L/H being 46.5 and 59.0 for underflow and overflow respectively. For the shortest lock length, $L_0/H = 1.8$, the travel of the underflow at T/T_Δ of 100 is reduced, but only to L/H of 35, although the subsequent reduction in non-dimensional distances covered at the standard non-dimensional times becomes increasingly marked.

In the region of viscous scale effect the underflow results consistantly show an irregularity which appears to be caused by the differing interaction of viscous damping of the fronts progress and of the pursuit of the front by the reflection as between different values of L_0/H and at different values of $(g')^{1/2}\ H^{3/2}/\nu$. Figure 14 shows comparison of the T/T_Δ lines of 10, 100, 1,000 and 10,000 for the various underflow diagrams. It will be seen that the onset of Froudian conditions with increasing value of $(g')^{1/2}\ H^{3/2}/\nu$ is delayed by decreasing value of L_0/H—which is explained by the decreasing potential energy available at the start of the experiment.

There is much less data for the overflow. The experimental difficulties at small values of $(g')^{1/2}\ H^{3/2}/\nu$ have been explained. At higher values of $(g')^{1/2}\ H^{3/2}/\nu$ the flume contained up to 2,000 kg of salt, and testing was restricted to the obtaining of confirmation that there were the same general trends as for the underflow, especially in the Froudian zone.

Effect of surface surges

In the experiments on which the new congruency diagrams are based, as in nearly all the previous experiments carried out by O'Brien and Cherno [12], Yih [13], Keulegan [11, 14] and by the author [1, 15], the same surface level has obtained on either side of the barrier before its removal. Thus upon removal of the barrier there is an unbalance of total force as shown in Figure 15 and the system responds by a mass movement of the fluid in addition to the initiation of exchange flow. A positive surge travels into the reach where the initial density is lesser and a negative surge travels into the reach where the density is greater. The surge velocities depend on the depth, and their relative magnitude and, consequent effect on non-dimensional front velocities, depends on the initial density difference. Figure 16 shows a surge system schematically.

It will be seen that in the circumstances of $(\rho_s - \rho)/\rho$ being relatively large, it is necessary to both maintain geometrical similarity in respect of both reaches of the flume, and to maintain $(\rho_s - \rho)/\rho$ constant, for similarity in front velocities to be attained, Figure 17 shows the results of such tests where the momentarily values of V_r/V_Δ have been computed with as great accuracy as possible.

Such surge effects have their own interest, but were something of an inconvenience with respect to the main objective of discerning viscous scale effect. The author was concerned with design of

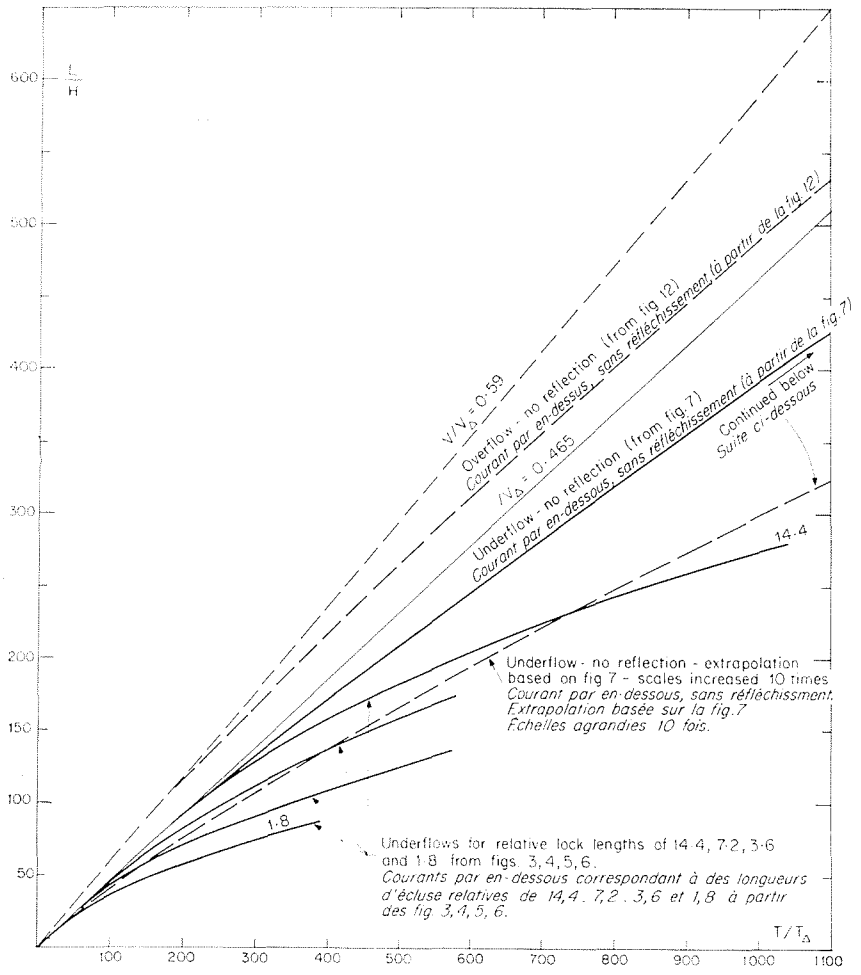

13/ Linear scale plots L/H against T/T_Δ outside range of viscous influence.

Variation de L/H en fonction de T/T_Δ en dehors de la zone d'influence de la viscosité.

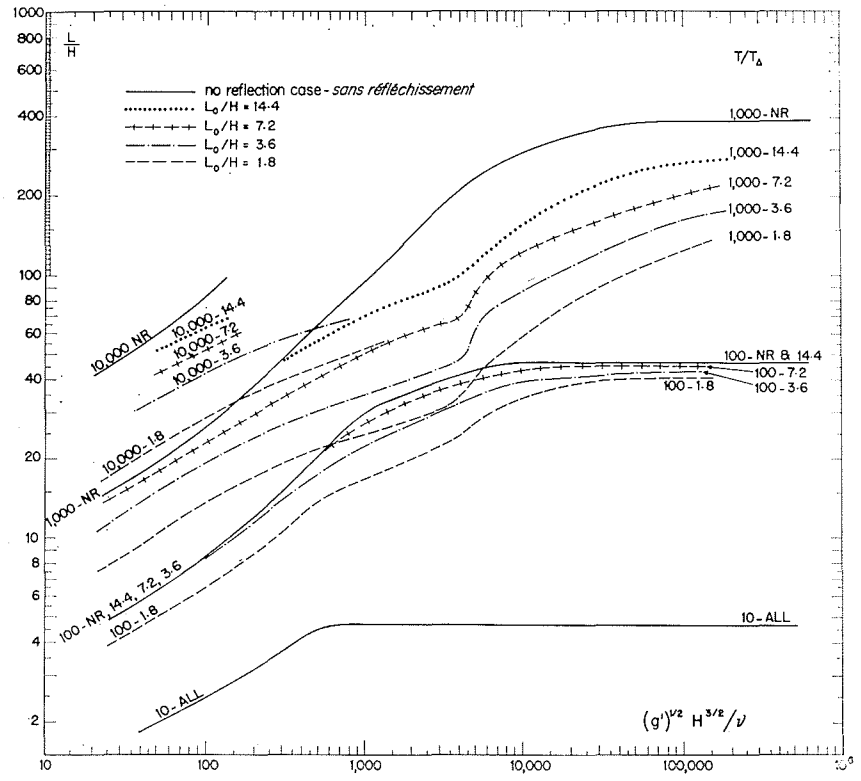

14/ Comparison of underflow results ($L_0/H = 14.4$, 7.2, 3.6 and 1.8, and no-reflection case).

Confrontation des résultats correspondants au courant par en-dessous ($L_0/H = 14.4$, 7.2, 3.6, et 1.8, et sans réfléchissement).

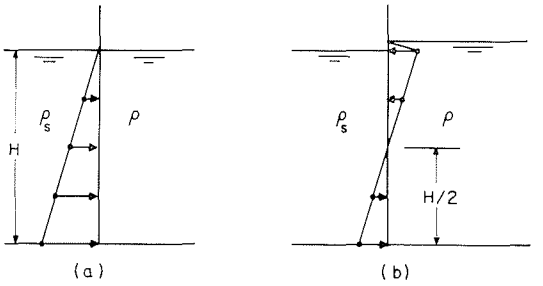

15/ Initial forces. *a)* Surface levels equal. *b)* Net force zero at mid-depth.

Efforts initiaux. a) *Cotes égales du plan d'eau.* b) *Effort net nul à mi-profondeur.*

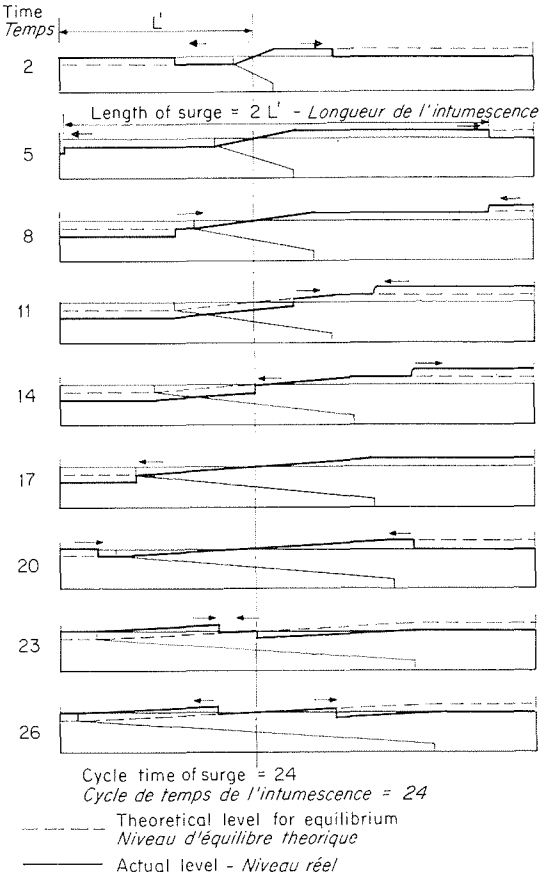

16/ Schematic illustration of surge system.

Représentation schématique du déroulement de l'intumescence.

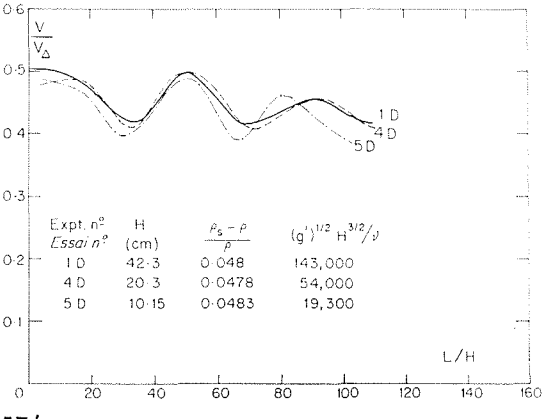

17/ Comparison of underflow front velocities with complete geometrical similarity.

Confrontation des vitesses du front du courant par en-dessous, en pleine similitude géométrique.

models studies where $(\rho_s - \rho)/\rho$ was often less than 0.005 and was the same in both model and prototype. To force the value of $(g')^{1/2} H^{3/2}/\nu$ obtained under the controlled conditions in the large flume, into the prototype region, it was desirable to use values of $(\rho_s - \rho)/\rho$ up to 0.1. There were, in fact, four possible approaches to those experiments in which the effect of reflection was avoided by placing the barrier at approximately the mid point of the flume (as in Fig. 16).

(*i*) The experiments could be carried out in enclosed flumes with $(\rho_s - \rho)/\rho$ varying as was adopted for the circular flume experiments leading to Figure 2. This was hardly practicable; the circular flume some 6 m long and had to be tilted to allow complete filling. In addition no true free surface overflow results would have been obtained.

(*ii*) The experiments would be carried out under conditions of one geometry and with $(\rho_s - \rho)/\rho$ constant, as for the experiments leading to Figure 17. This would have eliminated the valuable results for relative extensions greater than about 150, which are shown in Figure 7.

(*iii*) To balance the initial forces, the elevation of the less dense water can be made greater than that of the more dense water [16, 17] (Fig. 15). This initially eliminates the negative surge into the reach containing the more dense water, and substitutes a positive surge, and *vice versa* in the reach containing the less dense water but with the recreation of conditions for the mass surge due to density difference and a level surface. Thus the net effect might come close to the elimination of surges [16]. This method was not, however, adopted for the main test series and has not been tested in detail, although a preliminary test indicated that surges could be virtually eliminated in this manner.

(*iv*) To retain equal surface levels and to check on the effects of surge which are most relevant at small extensions, by using a combined initial plot with short lock length experiments, where surge effects are minimal. This course was adopted.

Effect of flume width

Keulegan's experiments.

Mention has already been made of Keulegans experiments [11], which were the only previous comprehensive test series of lock exchange flows. Keulegan attained high values of $(g')^{1/2} H^{3/2}/\nu$ in narrow channels only, i.e. $B/H = 0.5$. Keulegan's results are given in the form of variation of non-dimensional velocity, V/V_0, with relative distance L/H where $V = K.V_\Delta$, and K is a constant of proportionality which Keulegan took to be 0.462, although he also suggested the possibility of slow variation of K with $(g')^{1/2} H^{3/2}/\nu$. Some of his results have been converted to the form now adopted by the author. At lower values of $(g')^{1/2} H^{3/2}/\nu$, $L_0/H = 14.4$ and $B/H = 4$, there is quite good agreement with the author's results (Fig. 3). There is also quite good agreement at higher values of $(g')^{1/2} H^{3/2}/\nu$ despite that $B/H = 0.5$, but not at lower values of $(g')^{1/2} H^{3/2}/\nu$ (20,000). This suggests that the decreasing of relative breadth delays the onset of Froudian conditions, but that once attained, the same relative distance is travelled in the same non-dimensional time whatever the relative breadth. Assurance is thus provided that the author's diagrams hold for infinite width conditions. Despite the reduction of B/H to 3.5 at the highest values of $(g')^{1/2} H^{3/2}/\nu$ the same Froudian conditions were attained as at lower values of $(g')^{1/2} H^{3/2}/\nu$ where B/H ranged up to 15.

It is further likely that detailed work on Keulegan's results and the new results would reveal something close to a general correlation, based on:

$$\frac{T}{T_\Delta} = \Phi\left(\frac{\sqrt{g'H}}{\nu/R}, \frac{R}{H}, \frac{L}{H}\right) \qquad (12)$$

where R is a hydraulic mean depth. The present correlations are, of course, based on:

$$\frac{T}{T_\Delta} = \Phi\left(\frac{\sqrt{gH}}{\nu/H}, \frac{R}{H} \cdot \frac{L}{H}\right) \qquad (13)$$

and the author's are for the case of $R \doteq H$, while Keulegan's are for R considerably less than H (because $B/H = 0.5$). Brief checks indicate that, taking R as the conventional hydraulic mean depth for the whole waterway section i.e. $BH/(2H + B)$, the dependence on R/H in Eq. (13) is considerably reduced from that in Eq. (12).

The design method for model studies involving horizontal convective spread

The modified design procedure.

The initial premise is, firstly, that there will be scale effect in respect of the convective aspects of a surface (or bottom) horizontal convective spread, if small scale model simulation is attempted. This was clearly shown by the author [15], working between two systems of different size, albeit that both were within the region of viscous scale effect. Secondly, that there now exists fairly complete data on limits of spread for one type of purely convective spread. Since this data extends into the region of freedom from viscous scale effect, the region in which prototype occurrences will normally lie, it seems logical to take advantage of this knowledge.

It is necessary to proceed with the following points in mind.

1. As always [6] choice of vertical exaggeration is essentially for one prototype condition. This is not to say that other conditions will not be reasonably simulated, but the design computation is unique to one chosen condition.

2. Thus the prototype conditions should be chosen carefully so as to represent criticality in respect of the particular problem in hand.

3. There are, potentially, an innumerable number of conditions in lock exchange flow which

would require the same vertical exaggeration for correct simulation at the intended horizontal scale as applies to the actual phenomena to be modelled. But there is only one analogous lock exchange flow condition, wherein the onset of viscous scale effect will occur at the same reduction in natural scale as applies to actual phenomena of interest.

4. Thus the primary objective in the design method is to choose as nearly as possible this analogous lock exchange flow as the design condition.

Proceeding to an actual example, the method differs in detail from that previously given because of the new form of diagram now adopted. Suppose that it is assumed that the design lock exchange flow be of depth (H) 5 m, and of initial density difference ratio $(\rho_s - \rho)/\rho$ of 0.0015. This corresponds to a temperature rise of about 6 °C from 15 °C ambient in sea water. The median kinematic viscosity is approximately 1.1×10^{-2} cm²/sec; a prototype time of 1 hour is taken as design condition, corresponding, for example, to slack water in an estuary where semi-diurnal tides obtain.

This gives:

$$T/T_\Delta = 235$$

$$(g')^{1/2}\, H^{3/2}/\nu = 1.13 \times 10^6$$

and hence, using the no-reflection overflow case (Fig. 12):

$$L/H = 135 \qquad \text{at} \qquad T/T_\Delta = 235.$$

The horizontal scale has been selected as 1/350. It has already been shown that in a tidal model $(\rho_s - \rho)/\rho$ must be the same as in the prototype. The kinematic viscosity will not differ materially and the value of $(g')^{1/2}\, H^{3/2}/\nu$ for the natural model lock exchange flow will be that of the prototype divided by $350^{3/2}$ i.e. the value is 174. It is not possible to give a corresponding value of L/H at T/T_Δ of 235 in the overflow case, and recourse is made to the underflow case (Fig. 7) whence:

$(g')^{1/2}\, H^{3/2}/\nu$	T/T_Δ	L/H
1.13×10^6	235	100
174	235	17

The underflow factor of failure of 6 cannot differ greatly from that which would result for the overflow had data been available. It is not claimed that this factor of failure would apply to a situation where there is an element of forced flow as well as an element of convective spread; however, the failure would still be considerable.

To examine the ameliorating effect of vertical exaggeration, the overflow diagram (Fig. 12) can again be used—this latter covering the normal range of vertically exaggerated model practice. If the vertical exaggeration is e, the required relative extension obviously reduces to $135/e$. Now consider the effect of vertical exaggeration on the non-dimensional time. If the horizontal scale is $1/x$, and the vertical scale is $1/y$, i.e. $x/y = e$, then:

$$\left(\frac{T}{T_\Delta}\right)_m = \frac{T_p \times (\sqrt{y/x})}{\sqrt{\dfrac{H_p \times (1/y)}{[(\rho_s - \rho)/\rho]\, g}}} = \frac{T_p}{\sqrt{\dfrac{H_p}{[(\rho_s - \rho)/\rho]\, g}}} \times \frac{y}{x} \qquad (14)$$

i.e.:

$$\left(\frac{T}{T_\Delta}\right)_m = \left(\frac{T}{T_\Delta}\right)_p \times \frac{1}{e} \qquad (15)$$

where subscripts p and m refer to prototype and model respectively.

A trial and error procedure is now necessary; here this would lead to $e = 6.5$. Then the value of $(g')^{1/2}\, H^{3/2}/\nu$ in the vertically exaggerated model is $[(g')^{1/2}\, H^{3/2}/\nu]_p/(x/e)^{3/2}$ i.e. 2,800. Comparison of the values of the other non-dimensional groups is made below.

	$(g')^{1/2}\, H^{3/2}/\nu$	T/T_Δ	L/H
Prototype values.....	1.13×10^{-6}	235	135
Calculated values for 1/350 model with vertical exaggeration of 6.5.....	2,800	36	21
Values from figure 12.	at 2,800	at 36	20 Sufficiently close to 21

Thus we have for the model $1/x = 350$ and $1/y = 54$. A similar result would be obtained using the set of short lock length diagrams (Fig. 8 and 11). In this case, the relative lock lengths of 7.2, 3.6 and 1.8 necessarily represent vertical exaggerations of 2, 4 and 8 respectively as compared with the relative lock length of 14.4. Thus interpolation between diagrams would be necessary when data for an intermediate degree of exaggeration is required.

The procedure for calculation of required vertical exaggeration, in the case of simulation of an underflow phenomena, is entirely similar.

In fact, the solution obtained is unlikely to differ as between use of underflow and, alternatively, of overflow diagrams, once the design lock exchange flow circumstance has been determined.

It is emphasised that one seeks the minimum exaggeration to give the required extension in the model, because of the attendant disadvantages of distortion.

Criticism of design method.

The objective of the method is to obtain correspondence in limits of spread as between an actual prototype and its model. Criticism of the method can thus be considered under two distinct headings:

(*i*) Can the method attain the stated objective?

(*ii*) Is correspondence in limits of spread a sufficient objective?

Neither query can be completely answered at present but both delineate directions for further investigation.

Need for knowledge of other basic circumstances.

The author cannot but admit the need for a degree of knowledge of other circumstances which is at least comparable to that which now exists regard-

ing lock exchange flow; and at the same time emphasise that such knowledge does not appear to exist. Keulegan [18, 21] has provided much valuable data on the arrested wedge, but again mainly in relatively narrow channels. Ideally, a set of data on spread from a point source would complement data on linear extension. Even although this might be obtained in a segmental tank, quite large scale apparatus would be necessary to attain the region of freedom from viscous scale effect.

It is appropriate to emphasise the difference between the traditional pattern of calibration of a tidal model from known prototype data by adjustment of roughening, and the situation that obtains when simulation of convective surface spread is required. This latter aspect of the simulation of prototype phenomena is not amenable to calibration adjustment in the model and, indeed, it is quite likely that the phenomena to be simulated does not yet exist in the prototype. The scaling must be as correct as possible from the start, and there will always be a considerable element of judgment necessary in predicting the critical conditions to be expected in the prototype. Once the model prediction is available, the design method must be reapplied, with modification of the design lock exchange flow circumstance in the light of the model results. Only then can it be finally demonstrated whether there is a reasonable degree of compatibility between the predicted results and the chosen model scales so as to justify the acceptance of these results a representative of the prototype phenomena.

Need for knowledge of detail of lock exchange flow.

The second criticism is that, while the limits of spread may be correctly simulated, correspondence may not exist regarding important detail, such as the dilution, velocity structure and depths to interface.

There is a *prima facie* case that this criticism is unlikely to hold substance, because the design method is essentially based on bringing the flow phenomena which represents prototype occurrences in the vertically exaggerated model out of the range of viscous scale effect, as in the prototype. Nevertheless, obtaining of further data regarding the structure of lock exchange flow is obviously desirable.

Conclusions

1. Definitive data has been presented regarding the patterns of overall extensions of underflow and overflow in the wide channel condition of lock exchange flow. The data relates to a range of short lock lengths, including Keulegan's 14.4 and 7.2 relative lengths, and to the infinite length—no reflection case.

2. The author's hypothesis of onset of Froudian conditions with increasing absolute size of the phenomena has been confirmed.

3. The author's design method for simulation of convective spread in hydraulic model studies has been restated in terms applicable to the new form of congruency diagram which is now adopted.

4. The need for examination of the structure of lock exchange flow is emphasised.

5. A description of an actual hydraulic model study, where the principles and methods set out here were adopted, is to be published [22].

6. The author's method of synthesis is demonstrated to be a powerful device for the arrangement of variables in fluid mechanics problems. A treatment of the more intractable case of flume sediment transport is to be given [23].

Acknowledgements

The Science Research Council gave funds for the bulk of the equipment under a grant in aid of Laboratory and Field Studies of Density Difference Effects; The Clyde Port Authority provided accommodation for the long flume; Professor William Frazer, Head of Department of Civil Engineering and co-investigator for the S.R.C. grant, gave departmental support; Messrs. R. Lamb, A. Herdman, H. Allan, C. S. Chan and many others helped with the project. The Author is much indebted for this assistance.

References

[1] Barr (D. I. H.). — Densimetric exchange flow in rectangular channels. I: Definitions review and relevance to model design. *La Houille Blanche*, No. 7 (November, 1963).

[2] Barr (D. I.H.) and Hassan (A. M. M.). — Densimetric exchange flow in rectangular channels. II : Some observations of the structure of lock exchange flow. *La Houille Blanche*, No. 7 (November, 1963), 757-766.

[3] Majewski (W.). — The outfall of waste waters, including the effect of density differences. Laboratory investigations on the arrested wedge. *Proc. XIth Congress, International Association for Hydraulics Research*, Leningrad (1965).

[4] Discussion on paper: Effets des différences de température et de densité dans les circuits externes de refroidissement des centrales thermiques, by L. Mandelbrot. *La Houille Blanche*, No. 1 (1965), 58-60.

[5] Prandtl (L.). — The essentials of fluid dynamics. *Blackie*, London (1952).

[6] Barr (D. I. H.) and Shaikh (A. H.). — Model simulation of surface profiles in tidal and non-tidal water-courses. *The Engineer*, vol. 222, No. 5779 (October 28, 1966), 625-634.

[7] Barr (D. I. H.) and Smith (A. A.). — Application of similitude theory to the correlation of uniform flow data. *Proc. Inst. Civil Engineers*, vol. 37 (July 1967), 487-509.

[8] Barr (D. I. H.). — Similarity criteria for turbomachines. *Water Power*, vol. 18, No. 11 (November, 1966), 446-452.

[9] Barr (D. I. H.). — Density currents and public health engineering. *Water and Water Engineering*, vol. 70, No. 850 (December, 1966), 508-514.

[10] Rosensweig (R. E.). — The fascinating magnetic fluids. *New Scientist* (20 January 1966).

[11] KEULEGAN (G.H.). — Unpublished report: An experimental study of the motion of saline water from locks into fresh water channels. U.S. Dept. of Commerce, Nat. Bureau of Standards, Report No. 5168 (1957).

[12] O'BRIEN (M.P.) and CHERNO (J.). — Model Law for Motion of Salt Water Through Fresh. *Trans. American Soc. of Civil Engineers*, vol. 99 (1934), 576 (First published 1932 in Proceedings).

[13] YIH (C.S.). — Dynamics of nonhomogeneous fluids. *MacMillan*, N.Y. (1965).

[14] KEULEGAN (G.H.). — Unpublished report: The motion of saline fronts in still water. U.S. Dept. of Commerce, Nat. Bureau of Standards, Report No. 5813 (1958).

[15] BARR (D.I.H.). — Some observations of small scale thermal density currents. *Proc. 8th Congress I.A.H.R.* Paper 6 C, Montreal (1959).

[16] SCHIJF (J.B.) and SCHONFIELD (J.C.). — Theoretical considerations on the motion of salt and fresh water. *Proc. Minnesota International Hydraulics Convention, 5th Congress I.A.H.R.* (1953).

[17] BARR (D.I.H.). — Some Aspects of Densimetric Exchange Flow. *The Dock and Harbour Authority*, vol. 62, No. 494 (December, 1961).

[18] KEULEGAN (G.H.). — The mechanism of an arrested saline wedge. Estuary and Coastline Hydrodynamics, Ed. A.T. Ippen, *McGraw-Hill*, N.Y. (1966).

[19] KEULEGAN (G.H.). — Unpublished report: Interface mixing in arrested saline wedges. U.S. Dept. of Commerce, Nat. Bureau of Standards, Report No. 4142 (1955).

[20] KEULEGAN (G.H.). — Unpublished report: Significant stresses of arrested saline wedges. U.S. Dept. of Commerce, Nat. Bureau of Standards, Report No. 4267 (1955).

[21] KEULEGAN (G.H.). — Unpublished report: From characteristics of arrested saline wedges. U.S. Dept. of Commerce, Nat. Bureau of Standards, Report No. 5482 (1957).

[22] FRAZER (W.), BARR (D.I.H.) and SMITH (A.A.). — A hydraulic model study of heat dissipation at Longannet power station. To be published in *Proceedings, The Institution of Civil Engineers*, Vol. 38 (January, 1968), 23.

[23] BARR (D.I.H.) and HERBERTSON (J.G.). — Similitude theory applied to correlation of flume sediment transport data. To be published in *Water Resources Research*, American Geophysical Union.

Résumé

Courants de densité en canal rectangulaire
III. Expériences à grande échelle *

par D.I.H. Barr **

Introduction.

Le présent rapport fait suite à deux autres déjà publiés antérieurement dans *La Houille Blanche* [1, 2]. Il décrit des expériences à grande échelle sur les échanges ayant lieu à la suite de l'ouverture d'une vanne, qui ont été réalisées dans un nouveau canal long de 87,5 m, large de 152 cm, et permettant des hauteurs d'eau de fonctionnement allant jusqu'à 42 cm.

Méthode de synthèse appliquée aux phénomènes des courants de densité.

On établit des équations fonctionnelles sans dimensions à l'aide d'une nouvelle méthode de similitude [6-9]. On range d'abord les variables correspondantes dans une équation fonctionnelle dimensionnellement homogène à $(n + 1)$ termes, avant de les disposer au mieux, dans le but recherché, dans une équation fonctionnelle, sans dimensions, à n termes. En particulier, on peut avoir recours à la notion des vitesses dynamiques pour fournir des mesures de vitesse de l'effet des forces actives dans les systèmes à fluide accélérateur. On définit une vitesse dynamique comme étant proportionnelle à la vitesse atteinte lorsqu'un élément-type subit une force active sur une distance-type.

Dans le cas des échanges ayant lieu à la suite de l'ouverture d'une vanne d'écluse (fig. 1), la hauteur d'eau H est prise comme longueur-type. La forme active gravitaire réduite sollicitant un élément-type est proportionnelle à $(\rho_s - \rho)\, gH^3$, dans laquelle ρ_s correspond à la densité du liquide plus dense, et ρ à celle du liquide moins dense. La vitesse dynamique correspondant au mouvement de l'eau moins dense, V_Δ, est alors donnée par la relation :

$$V_\Delta = \sqrt{\left[\frac{(\rho_s - \rho)\, gH^3 \times H}{\rho H^3}\right]} = \sqrt{\left[\frac{(\rho_s - \rho)}{\rho}\, gH\right]} = \sqrt{g'H}$$

On montre que la vitesse dynamique visqueuse, V_ν, correspond à ν/H, ν étant la viscosité cinématique. En formant les mesures de vitesse dynamique, on peut éliminer toutes les constantes, puisqu'il s'agit de l'application conséquente des mesures à des systèmes comparables.

Courants d'échange dans une conduite circulaire.

L'auteur décrit des expériences effectuées dans des conditions de différence de densité élevée, et montre que l'on peut se permettre de négliger le groupe ρ_s/ρ dans la corrélation de la série principale d'expériences. Il examine l'in-

* Les deux premières parties de cette étude, (I : Définitions, connaissances actuelles, études sur modèle; II : Quelques expériences sur la structure de l'écoulement consécutif à l'ouverture d'une vanne) ont paru dans le n° 7-1963 de *La Houille Blanche*, p. 739 à 766.

** Department of Civil Engineering, University of Strathclyde, Glasgow.

fluence éventuelle de variations de la tension superficielle, des intumescences superficielles, et des groupes de corrélation.

Expériences sur les échanges dans les biefs de faible longueur.

Des résultats ont été obtenus pour le cas d'un canal de grande largeur, et pour des biefs de faible longueur relative $L_0/H = 14{,}4,\ 7{,}2,\ 3{,}6,\ 1{,}8$, à l'intérieur d'une gamme d'échelles absolues étendue, et étant déterminée par la valeur du second terme de l'équation adimensionnelle adoptée pour la corrélation (et indiquée ci-dessous), soit par la valeur du rapport entre les deux vitesses dynamiques correspondantes V_Δ/V_p :

$$\varphi\left(\frac{T}{\sqrt{(H/g')}}, \frac{(g'^{1/2}\,H^{3/2}}{\nu}, \frac{L}{H}\right) = 0$$

dans laquelle T correspond au temps écoulé après l'ouverture de la vanne et nécessaire pour que le front considéré parcoure une distance L de cette vanne.

Les résultats relatifs au courant inférieur ('underflow') sont indiqués sur les figures 3, 4, 5 et 6, correspondant à $L_0/H = 14{,}2,\ 7{,}2,\ 3{,}6,\ 1{,}8$; les résultats correspondants pour le courant supérieur ('overflow') sont indiqués sur les figures 8, 9, 10, 11.

Echange ayant lieu avec la vanne située à mi-longueur environ du canal.

Les résultats correspondant aux courants inférieur et supérieur sont indiqués, respectivement, sur les figures 7 et 12. Ces résultats ont été adoptés pour la méthode de calcul dont la description sera donnée par la suite.

Passage en similitude de Froude, et réduction des vitesses.

L'hypothèse de l'auteur quant au passage en similitude de Froude, lorsque la valeur du rapport V_Δ/V_p, croît, se trouve vérifiée. Cette hypothèse avait déjà fait l'objet d'une discussion publiée dans *La Houille Blanche* [4]. On examine les différents aspects de la diminution des vitesses. La figure 14 confronte les résultats essentiels.

Influence des intumescences superficielles.

L'auteur montre que l'influence des intumescences superficielles augmente de plus en plus à mesure que la valeur du rapport ρ_s/ρ augmente au-delà de l'unité.

Influence de la largeur du canal.

L'auteur confronte les résultats des présents essais et ceux des essais en canal étroit effectués par Keulegan [11].

Méthode de calcul pour les études sur modèle faisait intervenir l'étalement horizontal par convection.

La nouvelle forme du schéma de congruence rend nécessaire la révision de la méthode, mais non du principe, de la méthode de détermination d'échelle donnée précédemment! Un calcul-type est présenté comme exemple de l'application de la nouvelle méthode. On examine les aspects critiquables éventuels de la méthode.

Conclusions.

Des données définitives ont été présentées sur les configurations du développement des courants inférieur ('underflow') et supérieur ('overflow') dans un canal de grande largeur, dans des conditions d'écoulement d'échange consécutives à l'ouverture d'une vanne. L'hypothèse de l'auteur sur le passage en similitude de Froude, lorsque la grandeur absolue augmente, est vérifiée, et l'auteur présente une nouvelle définition de sa méthode de calcul de l'étalement par convection, en fonction du nouveau schéma de congruence maintenant adopté. La structure de l'écoulement d'échange consécutif à l'ouverture d'une vanne mérite un examen particulier. On indiquera par la suite des détails sur l'application de la méthode de calcul à une étude sur modèle proprement dite [22]. Enfin, l'auteur démontre que sa méthode de synthèse représente un puissant outil, permettant la disposition bien ordonnée des variables dans les problèmes de mécanique des fluides. On présentera également par la suite un traitement des cas les plus 'rébarbatifs' du transport des matériaux solides dans les canaux [23].